PCCP

PAPER

View Article Online
View Journal | View Issue

Cite this: *Phys. Chem. Chem. Phys.*, 2014, **16**, 22694

Spin–flip non-orthogonal configuration interaction: a variational and almost black-box method for describing strongly correlated molecules†

Nicholas J. Mayhall,[ab] Paul R. Horn,[ab] Eric J. Sundstrom[ab] and Martin Head-Gordon*[ab]

Received 26th June 2014,
Accepted 15th September 2014

DOI: 10.1039/c4cp02818j

www.rsc.org/pccp

In this paper, we report the development, implementation, and assessment of a novel method for describing strongly correlated systems, spin–flip non-orthogonal configuration interaction (SF-NOCI). The wavefunction is defined to be a linear combination of independently relaxed Slater determinants obtained from all possible spin–flipping excitations within a localized orbital active-space, typically taken to be the singly occupied orbitals of a high-spin ROHF wavefunction. The constrained orbital optimization of each CI basis configuration is defined such that only non-active-space orbitals are allowed to relax (all active space orbitals are fixed). A number of simplifications and benefits arise due to the fact that only a restricted number of orbital rotations are permitted, (1) basis states cannot coalesce during SCF, (2) basis state optimization is better conditioned due to a larger effective HOMO–LUMO gap, (3) smooth potential energy surfaces are easily obtained, (4) the Hamiltonian coupling between two basis states with non-orthogonal orbitals is greatly simplified. To illustrate the advantages over a conventional orthogonal CI expansion, we investigate exchange coupling constants of bimetallic complexes, the avoided crossing of the lowest singlet states during LiF dissociation, and ligand non-innocence in an organometallic complex. These numerical examples indicate that good qualitative agreement can be obtained with SF-NOCI, but dynamical correlation must be included to obtain quantitative accuracy.

1 Introduction

Hartree–Fock (HF) theory plays a foundational role in quantum chemistry. Defined as the best possible single determinantal wavefunction (in a variational sense), HF captures roughly 99% of the electronic energy for a given molecule. Often, however, it is the remaining 1% (called correlation energy) which provides the accuracy needed to reliably understand and predict chemistry.[1,2] For situations in which HF provides a qualitatively reasonable description of the electronic structure, quantum chemistry has a variety of methodological tools which can recover a desired amount of the correlation energy. The standard methods for computing correlation energy are Møller–Plesset perturbation theory (MP2, MP3, *etc.*), configuration interaction, CI, and coupled cluster theory.[3,4] Molecules containing multiple unpaired electrons or nearly degenerate electronic states, however, are generally outside the scope of applicability of these standard models. If more than one electronic configuration becomes significant, the mean-field description of HF breaks down, a result of so-called static, or strong correlation.[5]

The common course of action for treating systems with significant strong correlation is to identify an active space of orbitals and perform a complete active-space self-consistent field (CASSCF) calculation.[6] The complete active-space CI (CASCI) defines the determinant space corresponding to full CI among these active orbitals. For a unique specification for the orbitals, the CASCI energy is then variationally minimized with respect to both the CI and orbital coefficients. However, even though the resulting orbitals are optimal for the target eigenvector of the CASCI problem, they cannot be simultaneously optimal for all states. Higher energy states (obtained either through the CASCI eigenvectors or response theory[7]) will not be represented in a similarly optimal set of orbitals. While state-averaging attempts to provide a better balance, this inherently diminishes the ability of the method to correctly describe any individual state. In systems for which strong correlation arises due to interactions between configurations

[a] *Chemical Sciences Division, Lawrence Berkeley National Laboratory, Berkeley, California 94720, USA*
[b] *Kenneth S. Pitzer Center for Theoretical Chemistry, Department of Chemistry, University of California, Berkeley, California 94720, USA.*
E-mail: m_headgordon@berkeley.edu; Fax: +1 5106431255; Tel: +1 5106425957

† Electronic supplementary information (ESI) available: Cartesian coordinates of all complexes reported are provided. See DOI: 10.1039/c4cp02818j

of sufficiently different character, a single set of orbitals (*i.e.* HF or CASSCF) is often not sufficient for describing the CI basis necessary for a qualitative description of the problem.

To discuss this problem of CASSCF in more detail, let us consider a system composed of two unpaired electrons shared between two antiferromagnetically coupled metal centers in a closed-shell ligand field. In a localized orbital basis, each metal has one unpaired electron, and the spin-coupling of these two electrons yields two states: a biradical singlet and a triplet. If these were the only configurations in a CI expansion, then the triplet would always be lower in energy due to direct exchange. However, if one electron hops from metal A to metal B, then the resulting ionic closed shell configuration can mix with the biradical singlet (but not the triplet). If large enough, this mixing of the biradical singlet (covalent) and closed shell singlet (ionic) configurations can result in net antiferromagnetic coupling.

If CASSCF is used to compute either the covalent singlet or the triplet, the orbitals will be biased toward the covalent configuration. The ionic configurations in the CI expansion will then be poorly described, since large electrostatic effects would accompany a charge-transfer in the active space. Consequently, the CI determinants with significant ionic components will be unphysically high in energy, preventing any strong mixing with the covalent biradical singlet ground state. This effect has been well documented and explains, for the most part, why CASSCF underestimates exchange coupling constants in antiferromagnetic complexes so drastically.[8] Because the resulting CI weights of the ionic configurations are underestimated, internally contracted perturbative corrections to CASSCF (such as CASPT2), will also suffer from this same problem, since the PT2 effects cannot remix the zeroth order weights.[8]

Of course, a large enough CI expansion will recover all relaxation of the ionic configurations in addition to any other interaction. While uncontracted multireference CI (MRCI) methods provide a systematic way to improve the CASCI wavefunction, the high computational cost permits application to only the smallest systems. Perhaps the most accurate approach to computing exchange couplings has been difference dedicated CI (DDCI), which is an MRCI wavefunction chosen to consist of all determinants which have a non-zero second-order Hamiltonian coupling with the CASCI reference space.[9–12] Because each configuration in the CASCI expansion enjoys a full set of single (and higher) excitations, configuration-specific orbital relaxation effects are taken into account (in addition to differential dynamical correlation effects). However, the computational cost of a DDCI calculation prohibits application to large molecules/basis sets when several unpaired electrons are present. Other developments focus on incorporating the additional interactions by directly accessing larger active-spaces through a variety of means.[13–30] However, due to the complexity and cost of the currently available wavefunction methods, broken-symmetry DFT approaches are most often used, despite the large functional dependence, necessarily somewhat arbitrary projection formulas,[31–33] and high spin-contamination of computed determinants.

Non-orthogonal CI

Because the MRCI route of adding additional CI configurations to a CASCI wavefunction quickly becomes intractable, a minimal active space description with improved CI configurations is an attractive solution. Non-orthogonal CI (NOCI) provides a strategy for doing just this.[34–41] As a CI method, the NOCI wavefunction is defined as a linear combination of determinants, the weights of which are variationally optimized. However, in contrast to conventional CI, the determinantal basis used in NOCI needn't refer to a common set of orbitals. In previous papers, the non-orthogonal determinants used to define the CI expansion have come from either separate HF calculations,[40–43] or from state-interaction CASSCF (SI-CASSCF) calculations.[39,44] The reason NOCI is of interest for our current discussion is that, as demonstrated in the past,[37,39,44,45] NOCI provides the ability to improve the description of antiferromagnetic coupling by allowing the ionic configurations to be relaxed by separate SCF optimizations. Because the orbital relaxation preferentially stabilizes the ionic configurations, the mixing with the antiferromagnetic ground state can increase as a result. This provides a theoretically pleasing way to deal with the shortcomings of CASCI, without increasing the size of the CI basis.

However, despite the formal advantages of NOCI, there are several practical disadvantages:

- NOCI is more of a strategy than a method. The non-orthogonal determinants are generally hand-picked to represent the important physics for a specific problem. While this has the benefit of often needing rather short CI expansions, this is not helpful for defining a black-box method.
- Because the NOCI configuration space is usually defined as the result of multiple non-linear optimizations (SCF), it is often difficult to guarantee a dimension of the CI vector. Different SCF solutions may disappear or coalesce along a potential energy surface scan, resulting in energy discontinuities.
- Even when the desired SCF solutions exist, converging to them is typically more difficult than the ground state problem, since non-Aufbau ordering must be enforced.[46]
- Constructing the Hamiltonian matrix elements is significantly more difficult than with orthogonal determinants. For NOCI expansions containing more than just a few determinants, the Hamiltonian build quickly becomes the computational bottleneck.

Because of the ability of NOCI to provide an accurate, physically insightful, and short CI expansion, a method which builds upon the strengths of NOCI but does not suffer from the above difficulties is highly attractive.

Spin–flip CI

In contrast to both CASSCF and NOCI, spin–flip configuration interaction (SF-CI) provides a single reference strategy for describing strong correlation. In SF-CI, an electronic state with higher spin multiplicity is first obtained, followed by application of a CI operator which simultaneously excites and flips the spin ($\alpha \rightarrow \beta$) of one or more electrons, to yield a multiconfigurational wavefunction with the desired low spin quantum number, m_s. Several different

realizations of the SF-CI strategy have been developed.[47–57] Because a high-spin reference can often be found which is well described by a single determinant (when the strong correlation arises from coupling of unpaired electrons), the problem of finding a suitable set of orbitals becomes rather simple, and the high-spin UHF or ROHF orbitals provide an appropriate orbital basis to define the CI expansion. The key simplification arises from the fact that the high-spin reference forces the electrons in the weakest bonds to occupy orthogonal orbitals with parallel spin. In other words, the high-spin reference variationally selects out the most natural active-space orbitals, those which have partial occupancy. This realization has been leveraged to develop the set of active-space based spin-pure SF-CI methods, *i.e.*, spin-complete SF-CIS (SC-SF-CI), spin–flip extended configuration interaction singles (SF-XCIS), restricted active-space spin–flip (RAS-SF), SF-CAS(h,p), and SF-CAS(S).[51,53,54,57,58] All of these methods start with the CASCI wavefunction, with the active-space defined as the singly occupied orbitals coming from the high-spin ROHF determinant.‡ The CI wavefunction containing all spin–flipping excitations within the active space is referred to as spin–flip complete active-space CI (or SF-CAS).[57]

Although the spin–flip framework removes much of the difficulty encountered when specifying an active-space (with the only user specification being the multiplicity of the high-spin reference) SF-CAS is still hindered by the problems mentioned above for CASSCF. For the bimetallic example system discussed above, SF-CAS would use the orbitals from an ROHF triplet calculation and perform single spin–flipping excitations within the active space. This produces the four determinants (two ionic and two covalent)§ as described above. Because it is this purely covalent ROHF triplet state which is used to define the orbital basis, SF-CAS provides a very poor description of the ionic configurations, and, like CASSCF, the mixing with the ionic and neutral singlet configurations is drastically underestimated.

To address the missing orbital relaxation of the SF-CAS singlet states, SF-XCIS includes additional configurations which provide a full set of single excitations to each of the four SF-CAS determinants.[53] These single excitations describe configuration-specific orbital relaxation, and the resulting J coupling is enhanced. However, this significantly increases the computational cost compared to SF-CAS. Recently, we have developed a perturbative approximation to SF-XCIS, called SF-CAS(S),[58] which provides significant efficiency gains compared to SF-XCIS, and extends the applicability to multiple spin–flips. While the non-degenerate formulation of SF-CAS(S) provides significant improvements to SF-CAS, perturbation theory is not always sufficient, and non-negligible differences from the target SF-XCIS still remain.

In this paper, we present a new method based on both SF-CAS and NOCI, which we will refer to as spin–flip non-orthogonal CI (SF-NOCI). As discussed in the previous section, NOCI, while generally relatively accurate, suffers from problems related to definition and computational cost. SF-CAS, on the other hand, is computationally very simple and well defined but leaves much to be desired in terms of accuracy. SF-NOCI can either be regarded as a well-defined and simplified NOCI implementation, or rather, as an improved SF-CAS which is a CI expansion of partially relaxed determinants. Issues related to the definition, orbital optimization, and implementation are discussed below.

2 Methods

The SF-NOCI wavefunction is a linear combination of independently optimized determinants for which the expansion coefficients, c_w, are obtained variationally.

$$|\Psi^{\text{SF-NOCI}}\rangle = \sum_w c_w |\tilde{w}\rangle \quad (1)$$

In the above equation, $|\tilde{w}\rangle$ is a spin–flipped excitation from the ROHF reference determinant with the tilde indicating that the non-active-space orbitals have been relaxed for the wth active-space configuration. This state-specific orbital relaxation occurs by the following steps:

(1) Optimize the reference high-spin ROHF orbitals through conventional means.

(2) Generate a vector of α and β electron strings, to define the SF-CAS CI space. The electron strings simply define an electron occupation of the active-space orbitals.

(3) For each pair of elements of that α and β electron string vectors (this identifies a unique determinant), construct a guess molecular orbital coefficient matrix which reflects the occupancy for the corresponding electron strings. This simply shuffles the columns of the reference ROHF coefficient matrix to place the newly occupied orbitals into the occupied orbital block.

(4) For each initial guess coefficient matrix, perform a partial SCF optimization (preferably in parallel, since each SCF is independent of one another) whereby the active-space orbitals are unchanged. This only allows orbital rotations between two orbitals which are both outside of the active-space. We refer to this particular optimization as frozen active space SCF (or FAS-SCF).

The FAS-SCF is a constrained SCF optimization which allows only the non-active-space orbitals to relax under the influence of an effective external potential arising from the wth configuration's occupation of the active-space orbitals. To ensure that the final SF-NOCI wavefunctions are completely free of spin-contamination, the FAS-SCF procedure is performed in an RHF fashion, *i.e.*, α and β orbitals are restricted to be identical. A simple flowchart of the steps involved are shown in Fig. 1.

The FAS-SCF optimization is performed for each SF-CAS basis determinant to provide a better description of the individual basis determinants. Because this orbital relaxation changes the determinantal basis, the SF-NOCI energy is not invariant to orbital rotations within the ROHF orbitals. However, we view this as a feature. Since the motivating arguments which inspired the SF-NOCI method refer directly to a local orbital basis, we simply adopt the convention that the singly occupied ROHF orbitals are localized prior to generating the determinants

‡ While the singly occupied orbitals define what is referred to as the *natural* active-space, most of the active-space SF-CI methods allow for extended active spaces to be used.

§ SF-CAS is invariant to orbital rotations in the active space, so it is equally valid to use canonical or localized orbitals.

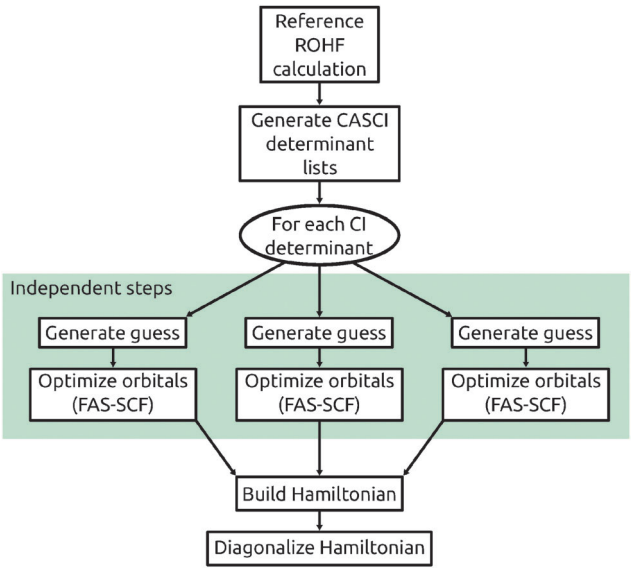

Fig. 1 Flowchart for the SF-NOCI method. Independent steps (shown in green) are uncoupled, and can be trivially parallelized.

relaxed by FAS-SCF optimization. If one were to use the non-local, canonical orbitals instead, very little orbital relaxation occurs, since these closed shell configurations are in-phase and out-of-phase combinations of the ionic configurations, which effectively cancel the large electrostatic components. In this initial implementation we have used the Boys localization,[59–61] though we plan to compare the various schemes in the future.¶ Because the active-space is treated with a full CI treatment, SF-NOCI is size-consistent. This has been verified numerically by computing both the super-system and isolated systems for the double bond dissociation of $CH_2{=}CHF$, with both localized and delocalized orbitals. Because it is an undressed Hamiltonian which is diagonalized, SF-NOCI is also variational. The SF-NOCI ground-state energy is guaranteed to be greater than (or somehow equal to) the exact energy.

Due to the fact that the active-space orbitals are unchanged during the FAS-SCF optimization, a number of simplifications arise:

• No two FAS-SCF optimizations can coalesce. Since the CI expansion within the active-space clearly does not contain duplicate configurations, each FAS-SCF is optimized in the presence of a unique and static active-space potential. This provides for a guaranteed CI dimension, and thus smooth potential energy surfaces are easily obtained.

• Each FAS-SCF optimization should be well-conditioned. One result of projecting out the active-space orbitals from the SCF equations is that the effective HOMO–LUMO gap is increased. This makes the optimization of the basis states faster and more reliable.

• All determinants are orthogonal. The determinantal overlap matrix needed in conventional NOCI is not needed. This ensures the rank of the SF-NOCI configuration space is equal to the dimension.

• Hamiltonian matrix elements can be obtained in a greatly simplified manner, since substitution patterns between the determinants can be predicted.

¶ We note that one could consider treating the orbital rotation parameters as a variational parameter, and optimizing the active-space orbitals simultaneously. However, this would significantly add to the complexity of the method, and it is not obvious that much would be obtained beyond using localized orbitals.

Computing Hamiltonian matrix elements

In order to evaluate the Hamiltonian matrix element between two determinants, w and x, each with their own one-electron orbitals, it is convenient to define a set of corresponding orbitals which can be obtained by performing a singular value decomposition (SVD) of their determinantal overlap matrix.[41]

$$\mathrm{SVD}({}^{w}\mathbf{C}_{\mu i}\mathbf{S}_{\mu\nu}{}^{x}\mathbf{C}_{\nu j}) = \mathrm{SVD}({}^{wx}\mathbf{S}_{ij}) = \mathbf{L}_{is'}\sigma_{s'}\mathbf{R}_{js'} \quad (2)$$

In the expression above, $\sigma_{s'}$ are the singular values, ${}^{wx}\mathbf{S}$ is the nonsymmetric determinantal overlap matrix, and $\mathbf{L}$ and $\mathbf{R}$ define the corresponding orbital transformations for the w and x determinants, respectively. The product of all singular values provides the overlap of the two determinants. However, because every basis determinant has a unique occupation of active space orbitals, and because these active-space orbitals are common to all basis determinants, the determinantal overlap is always zero.

$$\langle \tilde{w}|\tilde{x}\rangle = \det(\mathbf{L})\det(\mathbf{R})\prod_{s'}\sigma_{s'} = 0 \quad (3)$$

Furthermore, as a two electron operator, the Hamiltonian can only couple determinants which have up to two zeros in their list of $\sigma_{s'}$. In conventional NOCI strategies, one does not have obvious relationships between the determinants, and so any two determinants may overlap in any manner. In contrast, SF-NOCI has a great deal of structure created as a result of the constrained SCF optimization, and it is easily seen that any pair of determinants which differ among non-active-space orbitals will not contribute to the Hamiltonian. We consider the cases where w and x differ by one or two electrons (*i.e.*, the ${}^{wx}\mathbf{S}$ has one or two zero singular values) separately.

CASE 1: w and x differ by one electron

In NOCI, the matrix element between w and x that differ by one electron ($\sigma_{i'} = 0$) is given by[40]

$$\mathbf{H}_{wx} = \hat{S}\left(\sum_{j'}\frac{\langle i'j'\|i'j'\rangle}{\sigma_{j'}} + \mathbf{h}_{i'i'}\right), \quad (4)$$

where primes indicate corresponding orbital indices, and $\hat{S}$ is the reduced overlap defined as:

$$\hat{S} = \det(\mathbf{L})\det(\mathbf{R})\prod_{i'}\begin{cases}\sigma_{i'}, & \text{if } \sigma_{i'}\neq 0\\ 1, & \text{otherwise}\end{cases}. \quad (5)$$

In a conventional NOCI implementation, each $\mathbf{H}_{wx}$ element requires the direct computation of integrals in the corresponding orbital basis, which is most efficiently done by building a Fock-like matrix using an overlap-weighted density matrix (see ref. 40).

However, in our case, we can avoid most integral evaluations due to the structure created from the FAS-SCF. Each pair of determinants differs by at least one active-space orbital. Thus, if w and x differ by one orbital, it must be an active-space orbital. Therefore, eqn (4) can be rewritten as,

$$\mathbf{H}_{wx} = \hat{S}\left(\sum_{j'} \frac{\langle sj' \| tj' \rangle}{\sigma_{j'}} + \mathbf{h}_{st}\right), \quad (6)$$

where s and t represent reference ROHF singly-occupied (active-space) orbital indices. This greatly reduces the number of integrals needed, since the above expression contains only a quadratic number of integrals (assuming that the active-space doesn't grow with system size).

In terms of our implementation, we could simply compute and store the half-transformed integrals, $\langle s\mu \| t\nu \rangle$, in memory, and then transform the atomic-orbital (AO) indices to the specific corresponding orbital basis for the w, x pair. Alternatively, we precompute a set of Fock-like matrices from the pseudo-density matrix, $\mathbf{P}^{st}$, for each pair of active-space orbitals, s, t, where,

$$\mathbf{P}^{st}_{\mu\nu} = \mathbf{C}^{0}_{s\mu}\mathbf{C}^{0}_{t\nu}. \quad (7)$$

The Hamiltonian matrix element is then obtained by contracting the appropriate Fock-like matrix with an overlap-weighted density matrix as in ref. 40.

CASE 2: w and x differ by two electrons

The two electron substitution case is rather straightforward after realizing that if two determinants differ by two orbitals, they must both be active-space orbitals.

This is most easily seen by considering the possibility that only one of the two orbitals is in the active-space. This means that the second orbital must be in the non-active-space doubly occupied orbitals. However, since the non-active occupied orbitals are restricted to remain doubly occupied, it can only have an even number of zero singular values, which would end up creating a total of three orbital differences between w and x, resulting in no Hamiltonian coupling.

The expression needed for the two electron substitution case is:

$$\mathbf{H}_{wx} = \hat{S}\langle st \| uv \rangle \quad (8)$$

which easily fits into memory, since s, t, u, and v are all active-space indices.

In contrast to previous methods which improve upon the SF-CAS wavefunction by introducing additional excitations, the SF-NOCI method retains the same CI dimension as the SF-CAS wavefunction. The restricted active-space spin–flip (RAS-SF),[54,56] include single excitations from doubly occupied orbitals into the active-space (hole states) and excitations of active-space electrons into the virtual space (or particle states). A full set of hole and particle excitations exists for each active-space configuration, and is included to describe orbital relaxation of the active space orbitals. In fact, these are exactly the degrees of freedom neglected in SF-NOCI (FAS-SCF relaxes only non-active orbitals). Thus a comparison between SF-NOCI and RAS-SF gives an indication as to which of the independent sets of orbital rotations is more important.

The SF-XCIS method,[53] on the other hand, includes all of the excitations in the RAS-SF method, plus all possible excitations from the doubly occupied space into the virtual space. SF-NOCI includes orbital mixing between the doubly occupied and virtual orbitals, and thus SF-NOCI can obtain some of the same effects as SF-XCIS. However, SF-XCIS includes a completely uncontracted set of singles excitations, such that each active-space configuration has a full set of single excitations which can all mix together. The orbital rotations in SF-NOCI are however specific to a given basis determinant, and thus they only interact through the Hamiltonian coupling of the basis states.

The SF-NOCI method has a number of similarities to the recent work of Subotnik and coworkers.[62–64] Both SF-NOCI and the methods defined in their work, the variationally orbital-adapted and orbital-optimized configuration interaction singles (VOA-CIS and OO-CIS), improve excited state wavefunctions through the use of orbital relaxation. However, there are key differences which make the methods complementary. SF-NOCI is essentially defined using an orbital basis, the size of the active-space determines the CI basis of partially relaxed determinants. In contrast, the VOA-CIS and OO-CIS methods are defined according to choosing a certain number of CIS basis states. Additionally, the orbital optimization occurs in a different manner for the various approaches. Because SF-NOCI is defined using an active-space it is most appropriate for modeling strongly correlated systems, or low-lying excited states. Alternatively, the VOA-CIS/OO-CIS methods appear to be better suited for systems which do not have strong correlation, those for which a single reference HF ground state exist.

The SF-NOCI method is also quite similar to the breathing orbital valence bond method (BOVB), which allows the valence bond orbitals to relax separately for each Lewis structure.[65,66] One key difference between SF-NOCI and BOVB is that optimization of the active-space orbitals is performed in the latter. While the accuracy of appears to be better for BOVB, SF-NOCI has a number of computational advantages (particularly in the construction of the Hamiltonian) in addition to being a true molecular orbital method. Other related methods containing optimized orbitals for excited states also exist.[67–70]

3 Numerical examples

In the following several sections, we assess the SF-NOCI method for a variety of example systems. In addition to the strongly-correlated radical coupling discussed above, potential energy curves, and vertical excitation energies are also computed. Aside from the CASSCF calculations, all calculations are performed using a development version of QChem 4.2,[75] which made use of the Armadillo linear algebra package.[76] The state-averaged CASSCF calculations are obtained using the GAMESS package.[77,78] To ensure reliable basis state optimization, the DIIS[79,80] algorithm has been implemented for the FAS-SCF procedure.

Table 1 Exchange coupling constants for the structures shown in Fig. 3. All calculations used the VTZ basis set, and the appropriate high-spin ROHF state was taken as the reference state for each calculation

J (cm^{-1})	(a) Cu(II)	(b) V(IV)	(c) Cr(III)	(d) Fe(III)
SF-CAS	−20.1	+3.3	−45.1	−30.3
SF-NOCI	−45.5	−9.6	−62.9	−38.0
RAS-SF	−27.2	+1.1	−60.1	—
SF-XCIS	−86.7	−29.4	—	—
Experiment	−581/−398[a]	−107[b]	−225[c]	−117[d]

[a] Solid/solution Phases. Ref. 71. [b] Ref. 72. [c] Ref. 73. [d] Ref. 74.

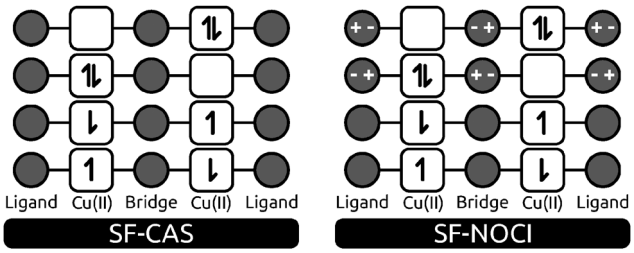

Fig. 2 Schematic comparison of the SF-CAS and SF-NOCI basis determinants. Plus and minus signs indicate charge polarization described by FAS-SCF procedure.

Bimetallic exchange coupling constants

The SF-NOCI method was motivated by a consideration of antiferromagnetically coupled bimetallic complexes. In this section, we provide four examples of spin-coupled transition metals, with the structures depicted in Fig. 3. For each of these systems containing weakly interacting radical centers, the low-energy electronic states can be mapped onto the spectrum of the phenomenological Heisenberg–Dirac–van Vleck Hamiltonian,[81–83]

$$\hat{H}^{\mathrm{HDVV}} = -2\sum_{ab} J_{ab}\hat{S}_a\hat{S}_b \qquad (9)$$

where J_{ab} is the isotropic exchange coupling constant between radical sites a and b, and $\hat{S}_a$ is the spin operator for center a only.‖ For the complexes in Fig. 3, only two radical sites exist and so only a single J value is needed. To relate theory to experimental data, a direct comparison of computed and experimentally fit J constants is usually made.

In Table 1, the exchange coupling constants, J, for each of the bimetallic complexes are reported for the SF-CAS, SF-NOCI, RAS-SF, and SF-XCIS methods, where applicable.

The first two of these complexes, **A** and **B**, each have a single unpaired electron on each metal center and therefore relate directly to Fig. 2. Both **A** and **B** have a single configuration triplet state, which is taken as the reference for the spin–flip calculations.

Considering **A** first, all four of the spin–flip methods predict the correct sign of J. As discussed above, the poor description of the ionic configurations results in SF-CAS predicting J values which are far too small in magnitude. Despite the fact that only non-active orbitals are allowed to relax in the FAS-SCF step, SF-NOCI creates a large effect on the magnitude of J, more than doubling it. This is in contrast to RAS-SF, which includes the effects of active-space orbital relaxation by way of single excitations. The RAS-SF values are significantly smaller than the SF-NOCI values, an indication that orbital relaxation is more important for core orbitals than for active-space orbital. SF-XCIS provides a better description, but at the cost of requiring a much larger CI space.

‖ Note that the isotropic $\hat{H}^{\mathrm{HDVV}}$ above specifically neglects the magnetic anisotropy resulting from the interaction with nuclear magnetic moments or spin–spin dipolar or spin–orbit coupling. While the exchange coupling constant is responsible for the main result of spin-state ordering, a description of magnetic anisotropy is ultimately required for a proper treatment of problems such as dioxygen activation,[84] or molecular magnetism.[85,86]

While all four methods predicted the correct sign for complex **A**, both SF-CAS and RAS-SF incorrectly predict complex **B** to be ferromagnetically coupled. Despite the qualitatively wrong SF-CAS starting point, SF-NOCI is able to recover the correct sign of J through orbital relaxation, though still non-negligibly smaller than the value obtained with SF-XCIS.

The third complex, **C**, contains two antiferromagnetically coupled Cr(III) centers, each with three unpaired electrons. The natural reference configuration for **C** is therefore the single configuration heptet reference with the desired M_s = 0 states obtained by three spin–flipping excitations. Although the number of configurations (400) present in the 3SF-NOCI calculation of **C** is significantly greater than the four configurations in the 1SF-NOCI (Fig. 2), the same arguments can directly be applied here. For **C**, both RAS-SF and SF-NOCI provide similar improvements to the SF-CAS description. Since this calculation requires three spin–flips, SF-XCIS is not applicable.

The fourth complex, **D**, contains two oxo-bridged Fe(III) centers, resulting in a minimal active-space size (neglecting double-shell effect) containing 10 electrons. Because the ROHF 11-et is the appropriate reference, direct application of any of these spin–flip methods would require five spin–flips. However, we have recently reported the success of using single spin–flip calculations for computing exchange coupling constants of multiradical systems.[87] This approach uses a mapping of the electronic Hamiltonian onto the HDVV Hamiltonian (eqn (9)), and enables the J constant to be derived from 1SF calculations, regardless of the number of electrons. While a 5SF-CAS calculation would certainly be possible with a code designed for large active-spaces, going beyond the simple SF-CAS description is much more difficult. SF-NOCI would demand over 63 000 SCF optimizations. Therefore, to compute **D**, we use the single spin–flip approach defined in ref. 87 to compute SF-NOCI J couplings with a CI expansion containing only 100 determinants. Here, SF-NOCI provides only a slight improvement over SF-CAS, with the enhancement being comparable in magnitude to that found for complex **B**.

A comparison to experiment clearly highlights the necessity for including dynamical correlation. All methods consistently underestimate the experimental values. However, SF-XCIS and SF-NOCI appear to be suitable approaches for achieving qualitative accuracy.

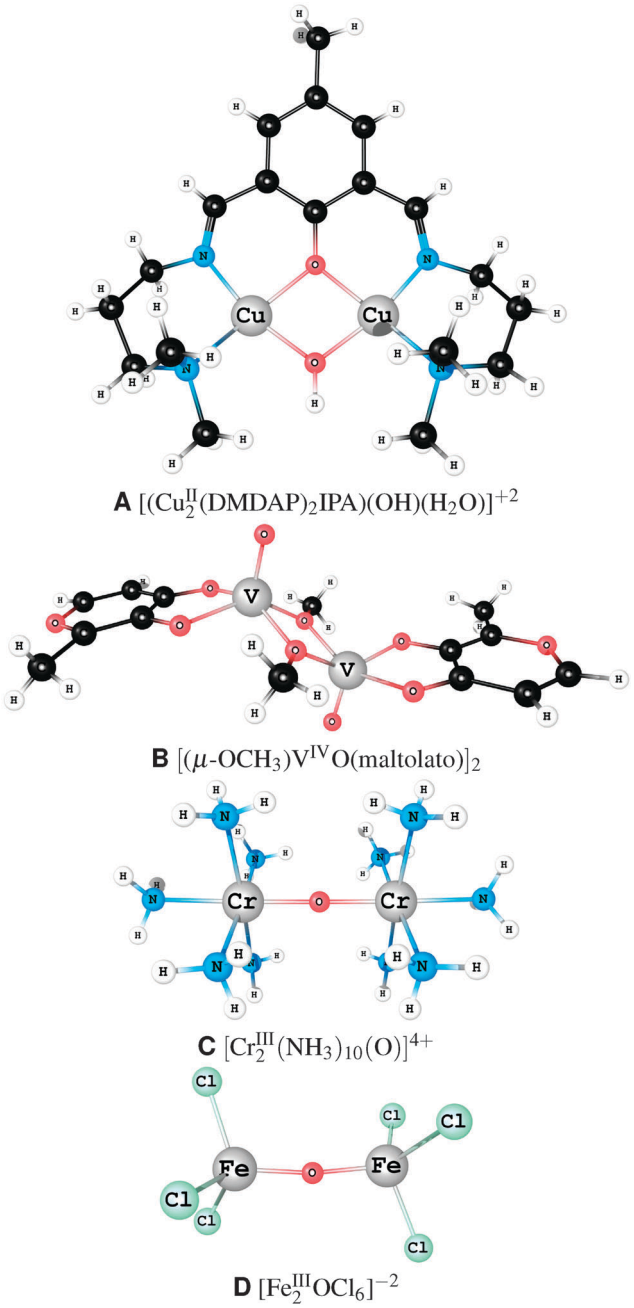

Fig. 3 Geometrical structures for the spin-coupled bimetallic systems. Each set of Cartesian coordinates was taken from experiment. **A** and **B** have two unpaired electrons, while **C** and **D** have 6 and 10 unpaired electrons, respectively.

Avoided crossings in LiF

To highlight the effect that orbital relaxation plays in the SF-NOCI method, we apply both SF-CAS and SF-NOCI to computing the avoided crossing of the two lowest $^1\Sigma^+$ states in LiF. A model example of quasidegeneracy, this system has been well studied and provides a strong justification for the current approach.[88–93]

Near the equilibrium, the ground state is well described by the $|1\sigma^2 2\sigma^2 3\sigma^2 4\sigma^2 1\pi^4\rangle$ configuration, which is ionic due to the dominant F(p_z) character of the 4σ orbital. The first excited $^1\Sigma^+$ state is predominately the spin-adapted, covalent $|1\sigma^2 2\sigma^2 3\sigma^2 4\sigma^1 1\pi^4 5\sigma^1\rangle$ configuration. As the bond length is stretched, the two states approach one another and, as required for states of the same symmetry in diatomic molecules, go through an avoided crossing.

In Fig. 4(a)–(c), the potential energy curves for the two lowest energy $^1\Sigma^+$ states are shown for SF-CAS, SA-CASSCF, and SF-NOCI. The ROHF triplet $|1\sigma^2 2\sigma^2 3\sigma^2 4\sigma^1 1\pi^4 5\sigma^1\rangle$ configuration was used for the reference, and a single spin flip was performed to obtain the desired singlet states. Since localized orbitals are used, the basis determinants can be interpreted as quasidiabatic states, which facilitates analysis.[40] In Fig. 4, adiabatic curves are drawn with a solid black line, and the quasidiabatic curves (the diagonal entries of the Hamiltonian matrix in a localized orbital basis), are represented with red dashed lines.

As seen in Fig. 4(a), the zeroth-order SF-CAS potential energy surfaces are far from being qualitatively correct. Because the ROHF reference orbitals are optimized for the triplet state, which is purely covalent, the ionic configuration is very poorly described and actually lies above the covalent state throughout most of the surface, a qualitative failure of SF-CAS. The SA-CASSCF curve is also qualitatively poor, with discontinuities which have been discussed in detail previously.[94,95]

When the orbitals are localized and relaxed, FAS-SCF completely reorders the approximate diabatic curves in SF-NOCI to achieve a qualitatively accurate description. However, the avoided crossing is much too soft and early. Experimentally, this should occur around 7.2 Å.[96] This is a result of the lack of dynamical correlation, which would preferentially stabilize the ionic state, delaying the avoided crossing and necessarily weakening the coupling of the two states, thereby making the avoided crossing sharper. The addition of dynamical correlation to the SF-NOCI model is currently being investigated.

Metal–ligand spin coupling

Organometallic complexes with ligands that actively participate in redox chemistry or interact with the metal *via* exchange interactions are referred to as non-innocent ligands. Consequently, it is often difficult to clearly define the oxidation state of the central transition metal in such complexes. For situations in which the transition metal is ferro/antiferromagnetically coupled to the ligand, the spin–flip methodology is well poised to provide a balanced description of the low-lying electronic states.

The complex in Fig. 5 provides an example of ligand-non-innocence.[97] Here, a Cu center is in a distorted tetrahedral field and assumed to be in a +2 oxidation state, giving it a d^9 configuration with a single unpaired electron. As the complex is overall neutral, the two ligands on the left and right are each in a −1 oxidation state, which implies that they too have a single unpaired electron each. With three unpaired electrons in such close proximity, three low-lying states will exist, two doublets and one quartet. In the experimental paper, it was determined that the overall spin was a doublet. However, this

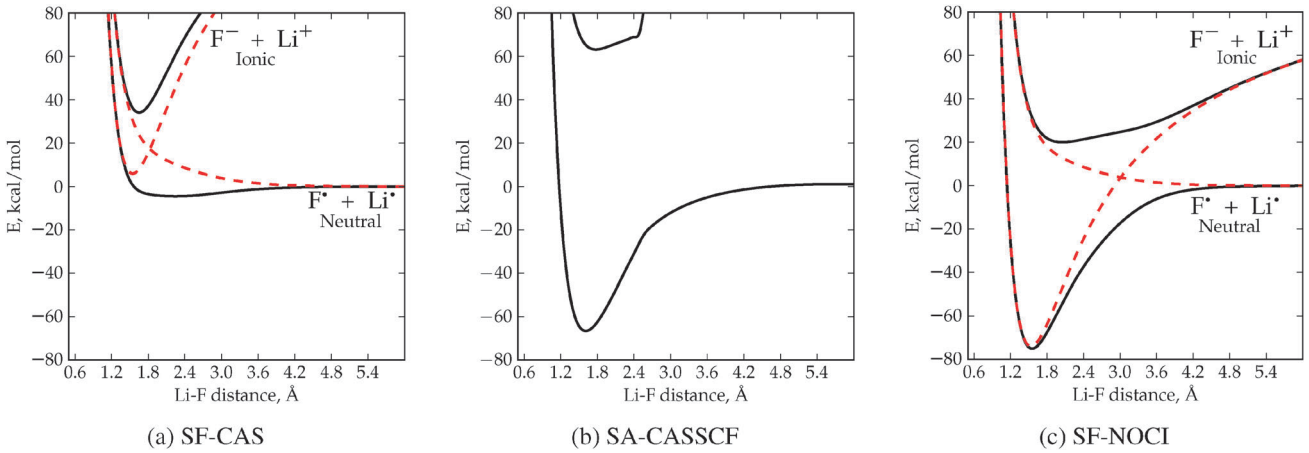

Fig. 4 Potential energy curves for LiF. Solid black curves are adiabatic states. Red dashed lines are the approximate diabatic curves (diagonal entries of the Hamiltonian in the localized orbital basis). State-averaged CASSCF diabatic curves were not obtained. The aug-cc-pVTZ basis set was used.

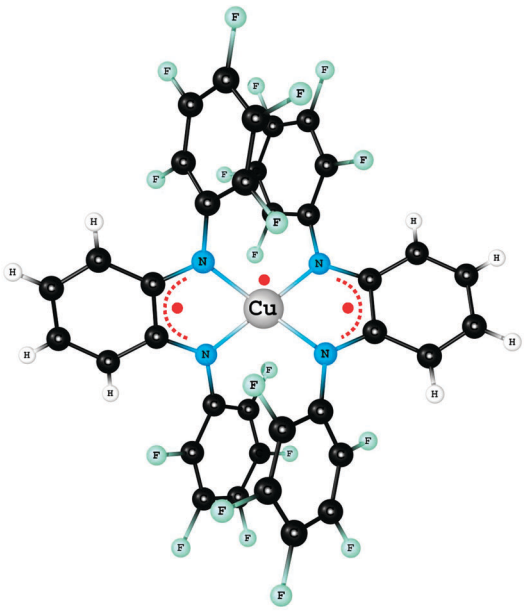

Fig. 5 Copper complex, $[Cu^{II}(^{F}sbqdi)_2]$, experimental structure from ref. 97. Red dots indicate unpaired electrons. Red dashed curves indicate delocalization of radical sites.

permits two distinct spin configurations, $|\uparrow\downarrow\uparrow\rangle$ and $|\uparrow\uparrow\downarrow\rangle$. The authors argued that because the long-range ligand–ligand coupling, $J_{L,L}$, must be smaller than the short-range metal–ligand couplings, $J_{Cu,L}/J_{L,Cu}$, $|\uparrow\downarrow\uparrow\rangle$ must be the dominant ground state configuration.

To study this system using spin–flip, it is apparent that one should take the high-spin ROHF quartet state as a reference. This puts all three strongly correlated electrons into orthogonal singly occupied orbitals, and the 1SF excitations give rise to nine determinants. In Table 2, we list the nine electronic states that result from diagonalizing the SF-CAS and SF-NOCI Hamiltonians. To compare to other SF-CAS based methods which have excitations outside of the active space, we include the SF-CAS(h,p) and SF-CAS(S) results. Because of the localization of the active-space orbitals, it is rather straightforward to characterize the spin configurations and the charge transfer character of the various excited states.

Qualitatively, all of the theoretical methods provide the same conclusion: that the $|\uparrow\downarrow\uparrow\rangle$ spin configuration is the ground state. This is in agreement with the experimental conclusions. The remaining two local excitations are also ordered similarly by all four methods. Considering all of the excited states, the following conclusions can be drawn:

- Compared to SF-CAS, SF-NOCI provides increased antiferromagnetic stabilization which is intermediate between the perturbative SF-CAS(h,p) and SF-CAS(S) values.
- For CT states, the stabilization affected by the FAS-SCF is very pronounced. The excitation energies of the CT states are reduced by nearly half, with the largest orbital relaxation effects providing over 6 eV of stabilization.
- Owing to the variational nature of the SF-NOCI method, higher energy states can be analyzed, whereas the perturbative approximation breaks down for SF-CAS(h,p) and SF-CAS(S), due to the well-known intruder state problems.

Although experimental excitation energies weren't available for comparison, the fact that SF-NOCI preferentially stabilizes the states with large charge-transfer character (and that this has large effects on the resulting adiabatic SF-NOCI CI states) illustrates that the behavior of the method is consistent with the discussion above. However, studies to further investigate the accuracy of SF-NOCI are currently underway.

Inter-site exchange coupling constants

Teasing out the various exchange coupling constants for a system with more than two radical centers is neither as straightforward, nor as well defined, as the bimetallic cases shown in Section 3. Multiple approaches have been defined,[98] and in this section we use a spectral decomposition to achieve this goal.[99]

In order to obtain the three J_{ab} interactions from eqn (9) (namely $J_{Cu,L}$, $J_{L,Cu}$, and $J_{L,L}$), one could use the off-diagonal elements of $\mathbf{H}$ between completely open-shell (or neutral)

Table 2 A comparison between SF-CAS and SF-NOCI for the vertical excitation energies of the organometallic complex in Fig. 5. Local excitations refer to the Heisenberg model-like states. States are described by labeling with either spin-up or spin-down or charged sites according to $|L_1ML_2\rangle$, where $L_{1,2}$ are the ligands, and M is the metal (Cu(II) in this case). LLIVCT are the ligand-to-ligand intervalence charge transfer excitations. LMCT are the ligand-to-metal charge transfer excitations. MLCT are the metal-to-ligand charge transfer excitations. The VTZ basis set was used for all calculations (962 basis functions)

Dominant configurations	Multiplicity	Character	SF-CAS	SF-NOCI	SF-CAS(h,p)	SF-CAS(S)
$\|\uparrow\downarrow\uparrow\rangle$	Doublet	Local	0.00	0.00	0.00	0.00
$\|\uparrow\uparrow\downarrow\rangle + \|\downarrow\uparrow\uparrow\rangle$	Doublet	Local	0.05	0.12	0.07	0.14
$\|\uparrow\uparrow\downarrow\rangle - \|\downarrow\uparrow\uparrow\rangle + \|\uparrow\downarrow\uparrow\rangle$	Quartet	Local	0.07	0.18	0.11	0.21
$\|+\uparrow -\rangle$	Doublet	LLIVCT	4.63	2.61	—	—
$\|-\uparrow +\rangle$	Doublet	LLIVCT	4.78	2.76	—	—
$\|\uparrow -+\rangle$	Doublet	LMCT	11.41	5.02	—	—
$\|+-\uparrow\rangle$	Doublet	LMCT	11.71	5.30	—	—
$\|\uparrow+-\rangle$	Doublet	MLCT	13.80	7.84	—	—
$\|-+\uparrow\rangle$	Doublet	MLCT	13.89	7.92	—	—

determinants in a localized orbital basis. However, these bare Hamiltonian matrix elements only contains the direct kinetic exchange integrals between a pair of sites, always favoring ferromagnetic ordering. Thus, rather than using the bare electronic Hamiltonian, we seek an effective Hamiltonian, $\mathbf{H}^{\text{eff}}$, which when diagonalized in the neutral determinant basis, provides identical eigenvalues for the low-energy spectrum of the SF-NOCI Hamiltonian.

To start, we first solve for the three lowest-energy eigenvalues (the local states in Table 2) of the SF-NOCI or SF-CAS electronic Hamiltonian,

$$\mathbf{HC} = \mathbf{CE}. \tag{10}$$

Because SF-NOCI contains all the possible configurations in the localized active-space, each eigenvector has both neutral ($\mathbf{C}_{\text{N}}$) and ionic ($\mathbf{C}_{\text{I}}$) components,

$$\mathbf{C}^{\text{T}} = \mathbf{C}_{\text{N}}^{\text{T}} \| \mathbf{C}_{\text{I}}^{\text{T}}. \tag{11}$$

However, the HDVV Hamiltonian, only acts on the neutral determinant space. Therefore, to obtain the effective Hamiltonian, we simply represent the three lowest-energy SF-NOCI eigenvalues in the basis defined by $\mathbf{C}_{\text{N}}$.

$$\mathbf{H}^{\text{eff}} = \tilde{\mathbf{C}}_{\text{N}} \mathbf{E} \tilde{\mathbf{C}}_{\text{N}}^{\text{T}} \tag{12}$$

Here, the tildes indicate that the neutral vectors have been symmetrically orthogonalized *via*,

$$\tilde{\mathbf{C}}_{\text{N}} = \mathbf{C}_{\text{N}} (\mathbf{C}_{\text{N}}^{\text{T}} \mathbf{C}_{\text{N}})^{-\frac{1}{2}} \tag{13}$$

The spectrum of $\mathbf{H}^{\text{eff}}$ is identical to the low-energy spectrum of the full *ab initio* electronic Hamiltonian, $\mathbf{H}$, and the off-diagonal elements now correspond to effective J_{ab} coupling parameters. The validity of $\mathbf{H}^{\text{eff}}$ can be ensured by observing a small norm in the orthogonal complement of the model space,

$$\text{tr}(\mathbf{C}_{\text{I}} \mathbf{C}_{\text{I}}^{\text{T}}). \tag{14}$$

In Table 3, we compare the J_{ab} values computed with the SF-CAS and SF-NOCI methods. Similar to the results presented in Section 3, SF-NOCI provides a significant enhancement of the exchange coupling for antiferromagnetically coupled radical centers. For each pair of sites, the J coupling is more than doubled, with the ligand–ligand coupling enhancing by a factor of nearly four. It is perhaps intuitive that the $J_{\text{L,L}}$ coupling would benefit the most from orbital relaxation since the lowest lying CT states are LLIVCT states. The same asymmetry between ligand sites seen in the CT states is observed also with the exchange couplings, *i.e.*, $J_{\text{Cu,L}} \neq J_{\text{L,Cu}}$.

Table 3 A comparison between SF-CAS and SF-NOCI for the computation of the intersite spin interactions of the organometallic complex in Fig. 5, as described by a Heisenberg Hamiltonian. The VTZ basis set was used for all calculations

J_{ab} (cm^{-1})	SF-CAS	SF-NOCI	SF-NOCI/SF-CAS
$J_{\text{Cu,L}}$	−231.0	−547.7	2.4
$J_{\text{L,Cu}}$	−164.8	−433.7	2.6
$J_{\text{L,L}}$	−9.4	−35.7	3.8

Due to the fact that the quartet was never populated in experiment, even at 300 K, the authors of that work concluded that the metal–ligand coupling must be much greater than 200 cm^{-1}.[97] Thus, the ordering of exchange couplings given was, $J_{\text{Cu,L}} \gg 200\ \text{cm}^{-1}$ and $J_{\text{Cu,L}} \gg J_{\text{L,L}}$.

While both SF-CAS and SF-NOCI correctly predict $J_{\text{Cu,L}} \gg J_{\text{L,L}}$, the magnitude of the $J_{\text{Cu,L}}/J_{\text{L,Cu}}$ couplings computed with SF-CAS, −231 and −165 cm^{-1}, do not agree with the experimental observations. Orbital relaxation plays a major role in this system, and the SF-NOCI couplings are all more than doubled, bringing the results into qualitative agreement with experiment.

4 Conclusions and future directions

SF-NOCI is presented with the intention of providing a clear-cut and efficient strategy for variationally improving CASCI (or SF-CAS) wavefunctions without resorting to increased CI expansions. By using a partial SCF optimization (referred to as FAS-SCF), the localized active-space configurations are allowed to relax *via* orbital optimization of the non-active-orbitals. Because only a limited number of orbital rotations are permitted in the FAS-SCF procedure, a number of advantages arise, as compared to full optimization (or straightforward NOCI):

• No two FAS-SCF optimizations can coalesce. This provides for smooth potential energy surfaces and a guaranteed CI dimension.

• Each FAS-SCF optimization should be well-conditioned. The effective HOMO–LUMO gap is increased, making the optimization of the basis states faster and more reliable.

• Building the SF-NOCI Hamiltonian matrix is much more efficient, since substitution patterns between the determinants are known a priori.

Compared to previous NOCI efforts, the current approach has significant definitional advantages requiring only a minimal amount of user input, namely the multiplicity of the high-spin ROHF reference. If this was guaranteed to always be a trivial task, the SF-NOCI would be a black box method. However, for situations in which a single configuration high-spin reference determinant is not easily obtained, care must be taken when defining the active-space.

For the antiferromagnetic coupling of bimetallic complexes, SF-NOCI increased the magnitude of J coupling compared to both SF-CAS and RAS-SF. For the V(IV) complex, both SF-CAS and RAS-SF incorrectly predicted ferromagnetically coupled centers, whereas SF-NOCI and SF-XCIS correctly obtained antiferromagnetic J coupling parameters.

The LiF dissociation was taken as an extreme example of the shortcomings of SF-CAS. Since the orbitals in the SF-CAS wavefunction come from the completely covalent triplet ROHF calculation, the ionic curve is far too high in energy, and the resulting adiabatic ground-state barely exhibits any molecular binding at all. By including variational orbital relaxation, SF-NOCI, recovers the correct qualitative description by stabilizing the ionic configurations, and the adiabatic curves exhibit the proper character and an avoided crossing, albeit at a far to early geometry due to the neglect of dynamical correlation.

An organometallic complex containing non-innocent ligands was also investigated. Excited states corresponding to the various excitations within the active space were considered, and the ability of SF-NOCI to stabilize charge-transfer states was illustrated. Additionally, by constructing an effective Hamiltonian and mapping to a Heisenberg spin Hamiltonian, we obtained the three intersite exchange coupling constants between the metal and two open shell ligands. Similar to the bimetallic cases, SF-NOCI provided significant enhancement of all three coupling constants, bringing the computed values into agreement with experimental estimates.

As mentioned above (and clearly obvious from comparing SF-NOCI to experimental values), dynamical correlation is the most important missing ingredient.

We expect the SF-NOCI method to provide a valuable tool for investigating problems such as exchange coupling or state mixing, one which relies neither on perturbation theory, nor extended CI expansions.

Acknowledgements

Support for this work was provided through the Scientific Discovery through Advanced Computing (SciDAC) program funded by the U.S. Department of Energy, Office of Science, Advanced Scientific Computing Research, and Basic Energy Sciences. Additional support was provided by the U.S. Department of Energy, Office of Basic Energy Sciences, Chemical Sciences, Geoscience, and Biosciences Division, through Contract No. DEAC02-05-CH11231.

References

1 J. Pople and J. Binkley, *Mol. Phys.*, 1975, **29**, 599–611.
2 *Adv. Chem. Phys.*, ed. I. Prigogine, John Wiley & Sons, Inc., Hoboken, NJ, USA, 1958, vol. 2.
3 C. Moller and M. S. Plesset, *Phys. Rev.*, 1934, **46**, 618–622.
4 J. Cizek, *J. Chem. Phys.*, 1966, **45**, 4256.
5 O. Sinanoglu, in *Adv. Chem. Phys.*, ed. I. Prigogine, John Wiley & Sons, Inc., 1964, pp. 315–412.
6 B. O. Roos, *Int. J. Quantum Chem.*, 1980, **18**, 175–189.
7 Y. Luo, D. Jonsson, P. Norman, K. Ruud, O. Vahtras, B. Minaev, H. Ågren, A. Rizzo and K. V. Mikkelsen, *Int. J. Quantum Chem.*, 1998, **70**, 219–239.
8 C. Angeli and C. J. Calzado, *J. Chem. Phys.*, 2012, **137**, 034104.
9 J. Miralles, J.-P. Daudey and R. Caballol, *Chem. Phys. Lett.*, 1992, **198**, 555–562.
10 J. Miralles, O. Castell, R. Caballol and J.-P. Malrieu, *Chem. Phys.*, 1993, **172**, 33–43.
11 C. J. Calzado, J. Cabrero, J. P. Malrieu and R. Caballol, *J. Chem. Phys.*, 2002, **116**, 3985.
12 C. J. Calzado, J. Cabrero, J. P. Malrieu and R. Caballol, *J. Chem. Phys.*, 2002, **116**, 2728.
13 D. Ma, G. Li Manni and L. Gagliardi, *J. Chem. Phys.*, 2011, **135**, 044128.
14 G. Li Manni, D. Ma, F. Aquilante, J. Olsen and L. Gagliardi, *J. Chem. Theory Comput.*, 2013, **9**, 3375–3384.
15 D. W. Small and M. Head-Gordon, *J. Chem. Phys.*, 2009, **130**, 084103.
16 D. W. Small and M. Head-Gordon, *Phys. Chem. Chem. Phys.*, 2011, **13**, 19285–19297.
17 D. W. Small and M. Head-Gordon, *J. Chem. Phys.*, 2012, **137**, 114103.
18 J. Cullen, *Chem. Phys.*, 1996, **202**, 217–229.
19 J. A. Parkhill, K. Lawler and M. Head-Gordon, *J. Chem. Phys.*, 2009, **130**, 084101.
20 J. A. Parkhill, J. Azar and M. Head-Gordon, *J. Chem. Phys.*, 2011, **134**, 154112.
21 J. A. Parkhill and M. Head-Gordon, *J. Chem. Phys.*, 2010, **133**, 124102.
22 J. A. Parkhill and M. Head-Gordon, *J. Chem. Phys.*, 2010, **133**, 024103.
23 T. Yanai, Y. Kurashige, E. Neuscamman and G. K.-L. Chan, *J. Chem. Phys.*, 2010, **132**, 024105.
24 S. R. White, *Phys. Rev. Lett.*, 1992, **69**, 2863–2866.
25 S. R. White, *Phys. Rev. B: Condens. Matter Mater. Phys.*, 1993, **48**, 10345–10356.
26 G. K.-L. Chan and D. Zgid, *Annu. Rep. Comput. Chem.*, 2009, **5**, 149–162.

27 G. Gidofalvi and D. A. Mazziotti, *J. Chem. Phys.*, 2008, **129**, 134108.
28 D. Mazziotti, *Phys. Rev. Lett.*, 2006, **97**, 143002.
29 D. A. Mazziotti, *J. Chem. Phys.*, 2007, **126**, 184101.
30 E. Neuscamman, *Phys. Rev. Lett.*, 2012, **109**, 203001.
31 L. Noodleman, *J. Chem. Phys.*, 1981, **74**, 5737.
32 J.-M. Mouesca, J. L. Chen, L. Noodleman, D. Bashford and D. A. Case, *J. Am. Chem. Soc.*, 1994, **116**, 11898–11914.
33 M. Nishino, S. Yamanaka, Y. Yoshioka and K. Yamaguchi, *J. Phys. Chem. A*, 1997, **101**, 705–712.
34 P.-O. Löwdin, *J. Appl. Phys.*, 1962, **33**, 251.
35 P. A. Malmqvist, *Int. J. Quantum Chem.*, 1986, **30**, 479–494.
36 R. Broer and W. C. Nieuwpoort, *Theor. Chim. Acta*, 1988, **73**, 405–418.
37 G. J. M. Janssen and W. C. Nieuwpoort, *Int. J. Quantum Chem.*, 1988, **34**, 679–696.
38 S. Matsumoto, M. Toyama, Y. Yasuda, T. Uchide and R. Ueno, *Chem. Phys. Lett.*, 1989, **157**, 142–145.
39 A. van Oosten, R. Broer and W. Nieuwpoort, *Chem. Phys. Lett.*, 1996, **257**, 207–212.
40 A. J. W. Thom and M. Head-Gordon, *J. Chem. Phys.*, 2009, **131**, 124113.
41 E. J. Sundstrom and M. Head-Gordon, *J. Chem. Phys.*, 2014, **140**, 114103.
42 P. Y. Ayala and H. B. Schlegel, *J. Chem. Phys.*, 1998, **108**, 7560.
43 S. R. Yost, T. Kowalczyk and T. Van Voorhis, *J. Chem. Phys.*, 2013, **139**, 174104.
44 R. Broer, L. Hozoi and W. Nieuwpoort, *Mol. Phys.*, 2003, **101**, 233–240.
45 H. Koch and E. Dalgaard, *Chem. Phys. Lett.*, 1993, **212**, 193–200.
46 A. T. B. Gilbert, N. A. Besley and P. M. W. Gill, *J. Phys. Chem. A*, 2008, **112**, 13164–13171.
47 A. Krylov, *Chem. Phys. Lett.*, 2001, **350**, 522–530.
48 A. I. Krylov, *Chem. Phys. Lett.*, 2001, **338**, 375–384.
49 A. I. Krylov and C. D. Sherrill, *J. Chem. Phys.*, 2002, **116**, 3194.
50 Y. Shao, M. Head-Gordon and A. I. Krylov, *J. Chem. Phys.*, 2003, **118**, 4807.
51 J. S. Sears, C. D. Sherrill and A. I. Krylov, *J. Chem. Phys.*, 2003, **118**, 9084.
52 S. V. Levchenko and A. I. Krylov, *J. Chem. Phys.*, 2004, **120**, 175–185.
53 D. Casanova and M. Head-Gordon, *J. Chem. Phys.*, 2008, **129**, 064104.
54 D. Casanova and M. Head-Gordon, *Phys. Chem. Chem. Phys.*, 2009, **11**, 9779–9790.
55 P. M. Zimmerman, F. Bell, M. Goldey, A. T. Bell and M. Head-Gordon, *J. Chem. Phys.*, 2012, **137**, 164110.
56 F. Bell, P. Zimmerman, D. Casanova, M. Goldey and M. Head-Gordon, *Phys. Chem. Chem. Phys.*, 2013, **15**, 358–366.
57 N. J. Mayhall, M. Goldey and M. Head-Gordon, *J. Chem. Theory Comput.*, 2014, **10**, 589–599.
58 N. J. Mayhall and M. Head-Gordon, *J. Chem. Phys.*, 2014, **141**, 044112.
59 S. Boys, *Rev. Mod. Phys.*, 1960, **32**, 296–299.
60 J. E. Subotnik, Y. Shao, W. Liang and M. Head-Gordon, *J. Chem. Phys.*, 2004, **121**, 9220–9229.
61 J. E. Subotnik, A. Sodt and M. Head-Gordon, *Phys. Chem. Chem. Phys.*, 2007, **9**, 5522–5530.
62 X. Liu, S. Fatehi, Y. Shao, B. S. Veldkamp and J. E. Subotnik, *J. Chem. Phys.*, 2012, **136**, 161101.
63 X. Liu and J. E. Subotnik, *J. Chem. Theory Comput.*, 2014, **10**, 1004–1020.
64 S. Fatehi, E. Alguire and J. E. Subotnik, *J. Chem. Phys.*, 2013, **139**, 124112.
65 P. C. Hiberty and S. Shaik, *Theor. Chem. Acc.*, 2002, **108**, 255–272, DOI: 10.1007/s00214-002-0364-8.
66 W. Wu, H. Zhang, B. Braïda, S. Shaik and P. C. Hiberty, *Theor. Chem. Acc.*, 2014, **133**, 1441.
67 H. Zhekova, M. Seth and T. Ziegler, *J. Chem. Theory Comput.*, 2011, **7**, 1858–1866.
68 T. Ziegler, M. Krykunov and J. Cullen, *J. Chem. Phys.*, 2012, **136**, 124107.
69 F. A. Evangelista, P. Shushkov and J. C. Tully, *J. Phys. Chem. A*, 2013, **117**, 7378–7392.
70 M. Krykunov, M. Seth and T. Ziegler, *J. Chem. Phys.*, 2014, **140**, 18A502.
71 A. Asokan and P. T. Manoharan, *Inorg. Chem.*, 1999, **38**, 5642–5654.
72 Y. Sun, M. Melchior, D. A. Summers, R. C. Thompson, S. J. Rettig and C. Orvig, *Inorg. Chem.*, 1998, **37**, 3119–3121.
73 E. Pedersen, *Acta Chem. Scand.*, 1972, **26**, 333–342.
74 G. Haselhorst, K. Wieghardt, S. Keller and B. Schrader, *Inorg. Chem.*, 1993, **32**, 520–525.
75 Y. Shao, L. F. Molnar, Y. Jung, J. Kussmann, C. Ochsenfeld, S. T. Brown, A. T. B. Gilbert, L. V. Slipchenko, S. V. Levchenko, D. P. O'Neill, R. A. DiStasio, R. C. Lochan, T. Wang, G. J. O. Beran, N. A. Besley, J. M. Herbert, C. Y. Lin, T. Van Voorhis, S. H. Chien, A. Sodt, R. P. Steele, V. A. Rassolov, P. E. Maslen, P. P. Korambath, R. D. Adamson, B. Austin, J. Baker, E. F. C. Byrd, H. Dachsel, R. J. Doerksen, A. Dreuw, B. D. Dunietz, A. D. Dutoi, T. R. Furlani, S. R. Gwaltney, A. Heyden, S. Hirata, C.-P. Hsu, G. Kedziora, R. Z. Khalliulin, P. Klunzinger, A. M. Lee, M. S. Lee, W. Liang, I. Lotan, N. Nair, B. Peters, E. I. Proynov, P. A. Pieniazek, Y. M. Rhee, J. Ritchie, E. Rosta, C. D. Sherrill, A. C. Simmonett, J. E. Subotnik, H. L. Woodcock, W. Zhang, A. T. Bell, A. K. Chakraborty, D. M. Chipman, F. J. Keil, A. Warshel, W. J. Hehre, H. F. Schaefer, J. Kong, A. I. Krylov, P. M. W. Gill and M. Head-Gordon, *Phys. Chem. Chem. Phys.*, 2006, **8**, 3172–3191.
76 C. Sanderson, *Armadillo: An Open Source C++ Linear Algebra Library for Fast Prototyping and Computationally Intensive Experiments*, Nicta technical report, NICTA, 2010.
77 M. W. Schmidt, K. K. Baldridge, J. A. Boatz, S. T. Elbert, M. S. Gordon, J. H. Jensen, S. Koseki, N. Matsunaga, K. A. Nguyen, S. Su, T. L. Windus, M. Dupuis and J. A. Montgomery, *J. Comput. Chem.*, 1993, **14**, 1347–1363.
78 M. Gordon and M. Schmidt, in *Theory Appl. Comput. Chem. first forty years*, ed. C. Dykstra, G. Frenking, K. Kim and G. Scuseria, Elsevier, 2005, ch. 41, pp. 1167–1189.

79 P. Pulay, *J. Comput. Chem.*, 1982, **3**, 556–560.
80 P. Pulay, *Chem. Phys. Lett.*, 1980, **73**, 393–398.
81 J. H. van Vleck, *The Theory Of Electric And Magnetic Susceptibilities*, Clarendon Press, Oxford, 1932.
82 W. Heisenberg, *Z. Phys.*, 1928, **49**, 619–636.
83 P. A. M. Dirac, *Proc. R. Soc. London, Ser. A*, 1926, **112**, 661.
84 R. Prabhakar, P. E. M. Siegbahn and B. F. Minaev, *Biochim. Biophys. Acta*, 2003, **1647**, 173–178.
85 S. Sinnecker, F. Neese, L. Noodleman and W. Lubitz, *J. Am. Chem. Soc.*, 2004, **126**, 2613–2622.
86 J. Cirera, E. Ruiz, S. Alvarez, F. Neese and J. Kortus, *Chemistry*, 2009, **15**, 4078–4087.
87 N. J. Mayhall and M. Head-Gordon, 2014, submitted for publication.
88 L. R. Kahn, *J. Chem. Phys.*, 1974, **61**, 3530.
89 E. Alguire and J. E. Subotnik, *J. Chem. Phys.*, 2011, **135**, 044114.
90 C. W. Bauschlicher and S. R. Langhoff, *J. Chem. Phys.*, 1988, **89**, 4246.
91 D. Casanova, *J. Chem. Phys.*, 2012, **137**, 084105.
92 L. Serrano-Andrés, M. Merchán and R. Lindh, *J. Chem. Phys.*, 2005, **122**, 104107.
93 H.-J. Werner, *J. Chem. Phys.*, 1981, **74**, 5802.
94 A. Sanchez de Meras, M.-B. Lepetit and J.-P. Malrieu, *Chem. Phys. Lett.*, 1990, **172**, 163–168.
95 A. Zaitsevskii and J.-P. Malrieu, *Chem. Phys. Lett.*, 1994, **228**, 458–462.
96 H.-J. Werner, *J. Chem. Phys.*, 1981, **74**, 5802.
97 M. M. Khusniyarov, K. Harms, O. Burghaus, J. Sundermeyer, B. Sarkar, W. Kaim, J. van Slageren, C. Duboc and J. Fiedler, *Dalton Trans.*, 2008, 1355–1365.
98 J. P. Malrieu, R. Caballol, C. J. Calzado, C. de Graaf and N. Guihéry, *Chem. Rev.*, 2014, **114**, 429–492.
99 J. des Cloizeaux, *Nucl. Phys.*, 1960, **20**, 321–346.